Point-Mutations Affecting the Properties of Tyrosine$_D$ in Photosystem II. Characterization by Isotopic Labeling and Spectral Simulation†

Cecilia Tommos,‡ Cathy Madsen,§ Stenbjörn Styring,*,‡ and Wim Vermaas‡,§

Department of Biochemistry, Arrhenius Laboratories for Natural Sciences, Stockholm University, S-106 91 Stockholm, Sweden, and Department of Botany and Center for the Study of Early Events in Photosynthesis, Arizona State University, Tempe, Arizona 85287-1601

Received May 3, 1994; Revised Manuscript Received July 11, 1994®

ABSTRACT: The reaction center of photosystem II (PSII) contains two redox-active tyrosines, Tyr$_D$ and Tyr$_Z$, which are Tyr160 and Tyr161 of the D2 and D1 proteins, respectively. We have introduced five site-directed mutations in the D2 protein in the vicinity of Tyr$_D$ to analyze the consequences of the mutations on spectral and functional properties of Tyr$_D^{ox}$. Characterization of three mutants, P161A and P161L (Pro161 changed to Ala and Leu, respectively) and Q164L (Gln164 mutated to Leu), is emphasized. Of these three mutants, only P161L is an obligate photoheterotroph; it is capable of oxygen evolution, but is photoinactivated rapidly. The D2 protein of this mutant migrates slower on a SDS–polyacrylamide gel. The EPR spectrum of Tyr$_D^{ox}$ is modified in the three mutants. The EPR spectra of Tyr$_D^{ox}$ in wild type and the mutants were characterized in detail by comparison of EPR spectra of thylakoids from cells grown in the presence and absence of tyrosine that was deuterated in specific positions. The experimentally obtained EPR spectra of wild type, P161A, and Q164L could be simulated satisfactorily using current theoretical models. The angle between one of the hydrogens on the β-methylene carbon and the $2p_z$ orbital at C_1 of the tyrosine ring was found to change slightly but significantly as a function of the mutations (52° in wild type, 50° in P161A, and 48° in Q164L). The overall electronic structure of Tyr$_D^{ox}$ is quite unaffected; only minor redistribution of the unpaired electron spin is observed between the wild type and the mutated systems. In all three strains, the spin density is in the range from 0.34–0.38 at carbon atom C_1, –0.08 at C_2 and C_6, and 0.26–0.29 at C_4 and the oxygen. In the P161L mutant a dark-stable, wide radical is observed with an intermediate g value (g = 2.0042). This EPR spectrum is also sensitive to tyrosine deuteration. However, the EPR spectrum is not easily understood in terms of a single Tyr radical and could not be simulated adequately. Possible reasons for this are discussed. Nonetheless, the results presented here imply the sensitivity of EPR spectroscopy to monitor changes in geometry and spin distribution in radicals as a function of alterations in their immediate protein environment.

In a number of biological systems, tyrosyl residues and tyrosyl-derived residues have been recognized to be involved in electron transport (Barry, 1993; Sigel & Sigel, 1994, and references cited therein). Detailed studies of oxidizable tyrosyl residues are facilitated in systems where oxidation is easily induced and where the oxidized radical remains stable for a relatively long time. These requirements are fulfilled by Tyr$_D$, the tyrosyl residue at position 160 of the D2 protein (Barry & Babcock, 1987; Vermaas et al., 1988a; Debus et al., 1988a), one of the reaction center proteins of photosystem II (PSII). Tyr$_D$ is easily oxidized by a short illumination and remains stable for hours in its radical form (Babcock & Sauer, 1973; Vass & Styring, 1991).

PSII catalyzes the light-induced reduction of plastoquinone and oxidation of water. The PSII reaction center is composed of two functionally central proteins, D1 and D2, which share significant sequence homology and have a similar secondary structure. Each of these proteins carries a redox-active tyrosyl residue at homologous positions in the third membrane-spanning region of the polypeptide [for reviews see Andersson and Styring (1991), Vermaas & Ikeuchi (1991), and Vermaas et al. (1993)]. The residue in the D1 protein, Tyr161 (Debus et al., 1988b; Metz et al., 1989), is the immediate electron donor to P680, which is the PSII reaction center chlorophyll. This tyrosyl residue, named Tyr$_Z$, is oxidized on the ns–μs timescale by P680$^+$ and is re-reduced by the water-oxidizing complex of PSII within 50 μs–1 ms [reviewed in Babcock (1987) and Rutherford (1989)]. In its oxidized form, Tyr$_Z$ gives rise to a characteristic EPR spectrum denoted signal II$_{vf}$ with "vf" standing for very fast, referring to its redox kinetics (Blankenship et al., 1975). If the water-oxidizing complex has been inactivated, reduction of Tyr$_Z^{ox}$ is slowed down considerably and the EPR spectrum, which is not altered in shape but decays with slower kinetics, is referred to as signal II$_f$ with "f" standing for "fast" (Babcock & Sauer, 1975).

The homologous tyrosyl residue in the D2 protein, Tyr$_D$, undergoes much slower redox kinetics. Oxidation of Tyr$_D$ occurs on the time scale of 1 s and involves the higher oxidation states of the oxygen-evolving complex (Babcock & Sauer,

† This work was supported by the Swedish Natural Science Research Council and by a research grant from the National Science Foundation (DMB 93-16857). In Stockholm, W.V. was a visiting professor on a grant from the Swedish Natural Science Research Council.

* To whom correspondence should be addressed. Telephone: +46-8-16 24 20. Fax: +46-8-15 36 79.

‡ Stockholm University.

§ Arizona State University.

® Abstract published in *Advance ACS Abstracts,* September 1, 1994.

[1] Abbreviations: Chl, chlorophyll; D1, the D1 reaction center protein in photosystem II; D2, the D2 reaction center protein in photosystem II; ENDOR, electron nuclear double resonance; EPR, electron paramagnetic resonance; HEPES, 4-(2-hydroxyethyl)-1-piperazineethanesulfonic acid; MES, 4-morpholineethanesulfonic acid; P680, primary electron donor in photosystem II; PSII, photosystem II; SDS, sodium dodecyl sulfate; Tyr$_D$, tyrosine$_D$, Tyr160 on the D2 protein, accessory electron donor in photosystem II; Tyr$_Z$, tyrosine$_Z$, Tyr161 on the D1 protein, immediate electron donor to P680.

0006-2960/94/0433-11805$04.50/0

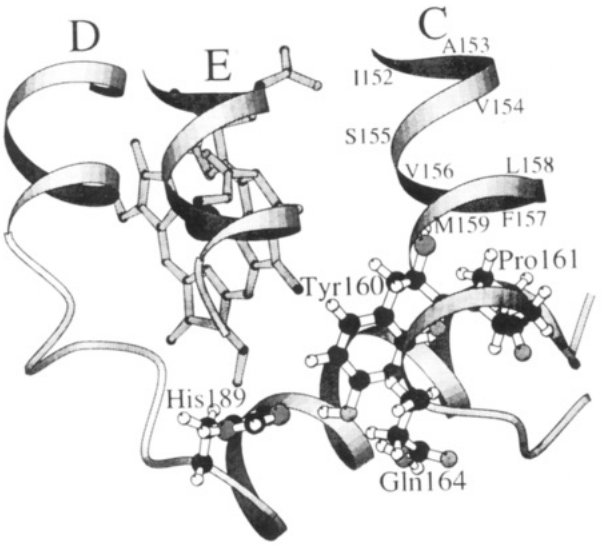

FIGURE 1: Structural model for the environment around Tyr_D on the lumenal side of the D2 protein in PSII. The figure shows part of the D2 protein with the plane of the membrane oriented perpendicular to the plane of the paper. The side chains of Tyr_D (Tyr160), His189, Gln164, and Pro161 (Tyr161, His190, Gln165, and Pro162 in higher plants) are drawn with "ball and stick" representation. The protein backbone, represented by wires, is placed as in the corresponding region of the structure of the bacterial reaction center from *Rhodopseudomonas viridis* (Deisenhofer et al., 1985). The figure is turned to show Pro161 clearly and includes the transmembrane helices C–E from the D2 protein. The figure also shows the CD helix in the lumenal loop between helices C and D, and one chlorophyll of the "special pair". The figure is created with the program MOLSCRIPT (Kraulis, 1991) and details of the model are published in Svensson et al. (1992).

1973; Vass & Styring, 1991). In its oxidized form, Tyr_D gives rise to an EPR spectrum that is very similar in line shape to the Tyr_Z^{ox} spectrum but that is stable for hours. It is therefore termed signal II_s, with "s" standing for slow (Babcock & Sauer, 1973). The midpoint redox potential of Tyr_D/Tyr_D^{ox} is between 700 and 800 mV (Boussac & Etienne, 1984; Vass & Styring, 1991). The extreme stability of Tyr_D^{ox} under physiological conditions is unusual and indicates that Tyr_D resides in a highly insulated protein environment (Babcock et al., 1989; Vass & Styring, 1991). This conclusion has been corroborated by structural modeling of the PSII reaction center that indicates that the structure around Tyr_D is very hydrophobic and efficiently shielded from the aqueous phase (Svensson et al., 1990, 1991; Ruffle et al., 1992).

The easily induced and highly stable Tyr_D^{ox} radical presents the opportunity to study the effect of the local protein environment on the properties of the radical and to determine residues that are in the immediate vicinity of Tyr_D. On the basis of the three-dimensional structure of the photosynthetic reaction center in purple bacteria (Deisenhofer et al., 1985), the three-dimensional structure of the protein surrounding Tyr_D has been modeled using homology-based computer modeling of PSII (Svensson et al., 1990, 1992; Ruffle et al., 1992). In addition, from ENDOR spectroscopy and spectral simulations, the hyperfine contributions to signal II_s, and thus the electronic structure of Tyr_D^{ox}, have been well characterized (Hoganson & Babcock, 1992, 1994; Rigby et al., 1994).

Using the structural model (Figure 1), the residues Gln164 and His189 of the D2 protein were predicted to be very close to the Tyr160 side group. In addition, a hydrogen bond between Tyr_D and His189 was proposed (Svensson et al., 1990). Mutations in these residues indeed were found to introduce significant modifications in the signal II_s line shape, confirming a close interaction. Most prominently, mutation of His189 to Leu or Tyr was found to lead to a loss of all fine structure in the signal II_s spectrum, while the functional properties of the radical did not change very much (Tommos et al., 1993). Independent studies also found that mutations of His189 to Gln and Asp result in large spectral modifications of signal II_s (Tang et al., 1993). The results presented in these studies (Tommos et al., 1993; Tang et al., 1993) support the existence of the earlier predicted hydrogen bond between Tyr_D and His189 (Debus et al., 1988a; Svensson et al., 1990).

Molecular information of how different mutations affect the properties of the tyrosyl radical will enhance our knowledge of protein–radical interactions in general. Therefore, it is important to analyze the EPR spectra of Tyr_D^{ox} in altered protein environments in detail. However, spectral analysis of signal II_s is complicated as the radical is immobilized in a nonoriented environment where anisotropy of the g and hyperfine tensors results in a broad and only partially resolved spectrum. Tyr_D^{ox} gives rise to a powder spectrum from which the magnitudes of the electron nuclear hyperfine interactions are difficult to determine. However, this problem can be addressed by *in vivo* deuteration of tyrosyl residues in combination with spectral simulation. Incorporation of isotope-labeled tyrosines can be achieved in the cyanobacterium *Synechocystis* sp. PCC 6803, the organism used in this study (Barry & Babcock, 1987). In the presence of exogenous Phe in the growth medium, the physiological biosynthetic pathway of aromatic amino acids is blocked but growth can be reestablished if tryptophane and tyrosine are added. The exogenously added aromatic amino acids are incorporated into newly synthesized protein, thus providing a means to label Tyr_Z and Tyr_D.

Isotopic labeling has proven to be a very useful technique in previous studies of Tyr_D^{ox} and tyrosyl radicals found in other proteins than PSII (Sahlin et al., 1978; Sjöberg et al., 1978; Bender et al., 1989; Boerner & Barry, 1993). Incorporation of fully deuterated tyrosines into *Synechocystis* 6803 showed that a tyrosyl radical was the origin of the EPR signal II_s (Barry & Babcock, 1987). Further studies, using tyrosines deuterated at specific sites, showed that the major hyperfine couplings responsible for the spectral line shape of signal II_s are those associated with the 3,5-hydrogens and the β-methylene hydrogens, while the couplings to the 2,6-hydrogens only have a very small effect on the spectrum (Barry et al., 1990).

In this paper, we have combined *in vivo* tyrosine deuteration with the use of mutants in which the environment of Tyr_D has been structurally altered. To characterize the altered spectral line shapes observed in the mutants, Tyr_D^{ox} was generated in samples containing tyrosines deuterated at specific positions. Furthermore, the fully protonated and specifically deuterated spectra have been simulated in order to determine the magnitude of the hyperfine contributions associated with the different hydrogens of the tyrosyl molecule. From the hyperfine tensors obtained, the geometry at the β-methylene position and the electronic structure for Tyr_D^{ox} in the different systems could be determined. The results indicate that the modified spectra observed, induced by structural perturbations around Tyr_D, generally can be explained by rotation of the phenoxy ring in combination with minor redistribution of the unpaired electron spin. We also report one mutation that was found to have a large effect on the whole system, also modifying the molecular properties of the D2 protein to a significant extent.

MATERIALS AND METHODS

Growth Conditions and Preparations of Thylakoid Membranes. Wild type and mutants of *Synechocystis* sp. PCC 6803 were cultivated in liquid BG-11 (Rippka et al., 1979) medium under continuous illumination (40 uE m^{-2} s^{-1}) at 32 °C in the presence of 5 mM glucose. When cultures were grown in the presence of exogenous tyrosine, filter-sterilized L-phenylalanine and L-tryptophan (dissolved in water) were added to the growth medium to final concentrations of 0.50 and 0.25 mM, respectively (Barry & Babcock, 1987). Due to the low solubility of tyrosine in water, tyrosine was added to the sterilized medium in powder form to a final concentration of 0.25 mM of the L-isomer. L-Tyrosine-(ring-3,5-D2) was purchased from Cambridge Isotope Laboratories. The isotopic purity of these compounds was 98%. DL-Tyrosine-$\beta\beta$-D2 was kindly provided by Dr. Björn Lindström.

Cyanobacterial cells were harvested by centrifugation, washed, and resuspended in preparation buffer containing 25 mM MES–NaOH, pH 6.5, 15 mM $CaCl_2$, 5 mM $MgCl_2$, 10% (v/v) glycerol, and 0.5% (v/v) dimethyl sulfoxide at a concentration exceeding 100 μg Chl mL^{-1}. After incubation for 1 h on ice, the cells were broken with an equal volume of 100 μm glass beads using a Mini-Beadbeater (BioSpec Products, Bartlesville, OK). The resulting suspension was diluted with 10 vol of preparation buffer containing 3 mM EDTA (to remove loosely associated Mn^{2+}). The glass beads were removed by sedimentation for 5–10 min on ice. The thylakoid membranes were pelleted by centrifugation at 25000*g* for 20 min at 4 °C and resuspended to a chlorophyll concentration of 2–3 mg mL^{-1}. The thylakoid membranes were frozen in liquid nitrogen and stored at –80 °C. The Chl *a* concentration was determined according to MacKinney (1941).

Site-Directed Mutations. Site-directed mutations were introduced into the D2 protein of *Synechocystis* 6803 by transformation of a *Synechocystis* strain lacking *psb*C (encoding CP43) and both copies of *psb*D (encoding the D2 protein) with a *psb*DI/C DNA construct carrying the desired mutation and a kanamycin-resistance cartridge downstream of the *psb*DI/C operon. Details on strains, plasmids, and methods have been described in Vermaas et al. (1990a). After generation of the desired *Synechocystis* mutants, the appropriate region of the *psb*DI gene was amplified from DNA isolated from these *Synechocystis* mutants. The amplified DNA was sequenced to verify the introduction of the desired mutation. For obligate photoheterotrophic mutants, the occurrence of secondary mutations that might inhibit PSII function was excluded by verifying that transformation with a 0.4 kb fragment of wild type DNA covering the site of the desired mutation could restore normal photoautotrophic growth. SDS polyacrylamide electrophoresis and Western blotting were performed according to Vermaas et al. (1988b). Before loading to the gel, the thylakoid samples were mixed with SDS at room temperature. The samples were not heated.

Quantification of Photosystem II on a Chlorophyll Basis. The amount of PSII reaction center in intact cells was determined by herbicide-binding assays using ^{14}C-labeled diuron (Amersham, Chicago, IL). The procedure for these measurements has been described by Vermaas et al. (1990b).

Oxygen Evolution. The oxygen-evolving activity of whole cells at saturating light intensity was measured using a Clark-type oxygen electrode (Gilson) at 30 °C in 25 mM HEPES, pH 7.0, with 0.5 mM 2,6-dimethyl-*p*-benzoquinone and 0.5 mM $K_3Fe(CN)_6$ as electron acceptors.

EPR Spectroscopy. EPR spectra were recorded and processed using a Bruker ESP300 X-band spectrometer. Measurements at 77 K were performed using a finger Dewar filled with liquid nitrogen. For EPR measurements below 77 K, the spectrometer was equipped with an Oxford Instruments liquid helium cryostat and a temperature controller. Relative spin concentrations on a chlorophyll basis in the wild type and in site-directed mutants of *Synechocystis* 6303 were determined by using the spectrum of Tyr_D^{ox} in the same preparation of PSII-enriched membranes from spinach (1 spin per 220–240 chlorophylls; Berthold et al., 1981; Miller & Brudvig, 1991; Nilsson et al., 1992) as a spin standard for all measurements. The EPR spectra, measured under nonsaturating conditions, were double-integrated using the ESP300 software, and the radical contents were calculated from their respective areas. To quantitatively oxidize Tyr_D, the samples were kept in room light for 5 min at room temperature (Vass & Styring, 1991) and then incubated in darkness for 3 min before freezing to allow reduction of $P700^+$, the oxidized primary donor of photosystem I that would otherwise interfere with the EPR spectra.

Simulation of the EPR Spectra. Simulation was performed using an updated version of a computer program, designed to simulate organic free radicals, originally described by Brok et al. (1986). The program was kindly provided by Dr. C. Hoganson, Michigan State University. To calculate a powder EPR spectrum, the program uses as parameters the principal values of the *g* and the hyperfine tensors along with the orientations of the hyperfine tensors with respect to the molecular *g* tensor. In our simulations we have used the anisotropic *g* values for Tyr_D^{ox} that have been determined in spinach by high frequency EPR measurements (g_x = 2.00752, g_y = 2.00426, g_z = 2.00212; Gulin et al., 1992). These *g* values, which so far have not been determined in cyanobacteria, were assumed to be constant between the different systems. For the simulation, the orientation of the *g* tensor was set similar to that of the radical in the tyrosine hydrochloride crystal (Fasanella & Gordy, 1969), with the largest value along the imaginary C_1–C_4–O axis (C_1 is the C atom of the ring covalently bound to C_β, and C_4 is the C directly attached to the O) and the smallest value perpendicular to the plane of the ring. The hyperfine couplings of the ring hydrogens were anisotropically simulated with noncoincident axis systems relative to the *g* tensor as in Hoganson & Babcock (1994). The simulated spectra were compared to the experimental spectra by visual inspection overlaying the spectra. The simulation parameters were adjusted by small increments of the variables until no further improvement of the simulated spectra could be obtained.

RESULTS AND DISCUSSION

Site-Directed Mutations. In this study, the following site-directed D2 mutants of *Synechocystis* 6803 were considered in detail: P161A (with Pro161 of the D2 protein changed to Ala), P161L [with Pro161 mutated to Leu; also see Vermaas et al. (1990c)], and Q164L, which carries a Gln164-to-Leu mutation and has been described earlier (Tommos et al., 1993). In addition, we have partially characterized two other mutants with changes at Pro161: P161S and P161R (with Pro161 changed to Ser and Arg, respectively). A model depicting residues 161 and 164 of the D2 protein relative to Tyr_D is provided in Figure 1. Prolines generally break the hydrogen bond pattern in a helix, and in this case Pro161 results in termination of the C helix three residues later at Gln164. Thus, mutations in Pro161 might facilitate structural rearrangements at the lumenal end of the C helix (Figure 1). In

Table 1: Characteristics of Site-Directed Mutants in *Synechocystis* 6803 with Alterations in the Vicinity of Tyr_D

	wild type	Q164L	P161A	P161L	P161R	P161S
Tyr_D^{ox}(spin/Chl)[a]	1/700	1/720	1/770	1/960	nd	nd
PSII/Chl[b]	1/780 ± 80	1/820 ± 90	1/850 ± 100	1/1620 ± 230	1/1200 ± 200	1/900 ± 100
photoautotrophic doubling time (h)	14	15	16	∞[d]	∞[d]	16
oxygen evolution (μmol O_2/(mg Chl)·h)[c]	322 ± 27	301 ± 32	289 ± 36	142 ± 31	215 ± 40	279 ± 28

[a] Spin quantification was performed by double integration of the EPR spectra and using Tyr_D^{ox} in the same preparation of PSII membranes from spinach as a spin standard. [b] The number of PSII reaction centers was determined from the number of diuron binding sites. [c] Oxygen evolution was measured in intact cells. [d] These strains are obligate photoheterotrophs and thus could not be maintained photoautotrophically.

addition, Pro161 is the residue next to Tyr_D, and mutations in this position may affect the radical. Gln164 is the final residue in the C helix. The side chains of Tyr_D and Gln164 are exposed on the same side of the helix (1 turn apart), and the two side chains point in approximately parallel directions. The side chains are expected to be in van der Waals contact with each other, ~3.5 Å apart (B. Svensson, personal communication). According to the model, Gln164 is one of the residues with the strongest interaction to Tyr_D, together with His189 and the residue at position 185, which is a Phe in higher plants and a Leu in cyanobacteria (Svensson et al., 1991). Thus, it is reasonable that a mutation at position 164 directly will affect Tyr_D.

The P161A, P161S and Q164L mutants grew photoautotrophically, with doubling times close to that of the wild type (Table 1). Their oxygen evolution capacity was also similar to that of the wild type (Table 1). In contrast, the P161L and P161R mutants were obligate photoheterotrophs and did not grow in the absence of glucose. Nevertheless, light-dependent oxygen evolution that was rapidly photoinactivated ($t_{1/2} \approx$ 1–5 min) could be observed (cf. Vermaas et al., 1990c). The levels of the oxygen evolution approximately reflected the PSII/Chl ratio in these mutants (determined from the number of herbicide binding sites; Table 1), suggesting that all PSII centers are fully active after dark adaptation. In P161A and Q164L, the number of PSII reaction centers on a chlorophyll basis was close to that in the wild type.

As these mutations may introduce structural changes in the D2 protein, the mobility of D2 was probed on a denaturing polyacrylamide gel. For this purpose, the gel was blotted and probed with antiserum raised against spinach D2. As shown in Figure 2, under the conditions used (a gel containing 6.5 M urea, and no heating of the SDS/sample mix), the D2 protein from wild type thylakoids mainly migrated as a 36 000 M_r band, with a band of lower intensity above it (at about 39 000 M_r). The immunoreaction with proteins around 68 000 M_r is routinely found in cyanobacterial thylakoids, and its origin is unclear. However, the 68 000 M_r components are unrelated to D2, as they are also evident in mutants lacking the genes coding for the D2 protein (Yu & Vermaas, 1993). The mobility of D2 as a 36 000 M_r band with a "smear" above it is in agreement with earlier studies [for example, see Eggers and Vermaas (1993) and Yu and Vermaas (1993)]. However, in the mutants, particularly in P161L, the 39 000 M_r band is much more prominent than in the wild type. In the P161L mutant only little of the lower band could be observed. Also under other gel electrophoresis conditions a significant difference in D2 mobility was observed, particularly between wild type and P161L (not shown). Large effects on protein mobility as a consequence of relatively small alterations in the primary structure have also been observed for the D1 protein (Kless et al., 1992). It thus seems clear that the P161L mutation has more severe effects on the structure and function of PSII than the other P161 alterations described in this study.

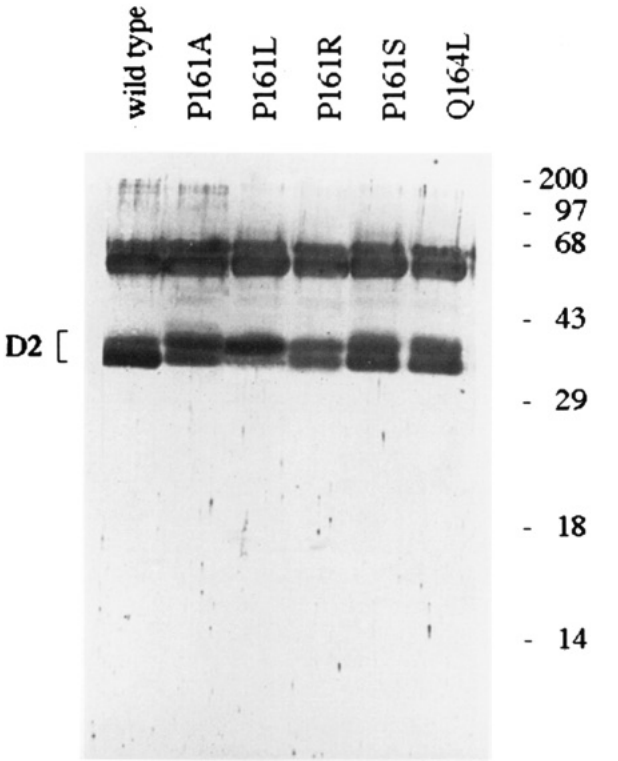

FIGURE 2: Western blot of thylakoid proteins from wild type and various mutants probed with rabbit polyclonal antibodies raised against the D2 protein from spinach. Lanes were loaded with thylakoid proteins from strains as indicated. The location and size of molecular weight markers has been indicated to the right. The amount of material loaded per lane corresponded to 2 μg of chlorophyll.

The reason for the obligate photoheterotrophic phenotype and the altered migration of the D2 protein in P161L as yet is unclear. Mutation of Tyr_D to a phenylalanine does not affect the photoautotrophic phenotype (Vermaas et al., 1988a; Debus et al., 1988a) even though the mutant grows slower. Also, P161A and P161S are photoautotrophs (Table 1). Therefore, a highly conserved sequence around the 160 position or a Pro residue at the 161 position of the D2 protein is not necessary for photoautotrophic growth. However, mutation of Pro161 to either Arg or Leu led to a mutant with a photoheterotrophic phenotype and containing a reduced but significant number of PSII centers (Table 1). It could therefore be inferred that it is impossible to accomodate a large residue at position 161 without a large structural effect on the D2 protein while smaller residues like alanine or serine interfere less with the structure and intactness of this part of PSII.

EPR Characterization of Tyr_D^{ox} in Wild Type and Mutants. Figure 3 shows low-temperature EPR spectra of thylakoid membranes from the wild type and site-directed mutants of *Synechocystis* 6803. The spectra of wild type, Q164L, and P161A can be conclusively assigned to Tyr_D^{ox} because they (1) were stable in darkness for extended periods, (2) showed spectral line shapes that are essentially identical to earlier

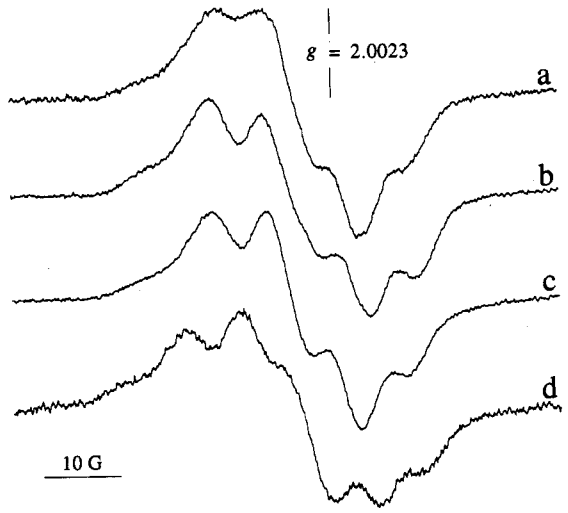

FIGURE 3: EPR spectra of Tyr_D^{ox} in thylakoid membranes from *Synechocystis* 6803 in the wild type (a), the Q164L mutant (b), and the P161A mutant (c). The dark stable signal observed in the P161L mutant is shown in d. The thylakoid concentrations were 2–3 mg Chl mL^{-1}. EPR conditions: microwave frequency 9.24 GHz (a,b) or 9.45 GHz (c,d); microwave power 6.3 μW (a,b) or 63 μW (c,d); modulation amplitude 1.6 G (a,b) and 3.3 G (c,d); gain, 5×10^5; time constant, 164 ms; spectral conversion time, 164 ms. The spectra were recorded at 10 K (a,b) or 77 K (c,d). Eight scans were added in spectra a and b while 30 scans were added in spectra c and d. Thus, the size of the spectra are not directly comparable.

published spectra of Tyr_D^{ox} from *Synechocystis* 6803 (Barry & Babcock, 1987; Vermaas et al., 1988a; Debus et al., 1988a), and (3) were modified as expected when cells were grown in the presence of specifically deuterated tyrosines (see below). The spectrum observed in the P161L mutant (Figure 3d) also resembled that of Tyr_D^{ox}. It was dark stable with a high g value and a broad line width. The spectrum was also modified when the mutant was grown with deuterated tyrosines. However, as will be discussed in a subsequent section, the spectrum recorded in thylakoids from the P161L mutant appeared to be more complex than the usual spectra from Tyr_D^{ox}.

The EPR signal originating from Tyr_D^{ox} in the wild type was a poorly resolved spectrum with a measured isotropic g value of 2.0050 and an overall peak-to-trough line width of 18 G (Figure 3a). When Gln164 of the D2 protein was mutated to Leu, the spectrum of Tyr_D^{ox} became slightly wider and exhibited a more resolved hyperfine structure as compared to the signal found in the wild type. The Tyr_D^{ox} spectrum of the Q164L mutant was 20 G wide with a g value of 2.0055 (Figure 3b; Tommos et al., 1993). The Tyr_D^{ox} spectrum of the P161A mutant (Figure 3c) was also somewhat modified as compared to that from wild type, with a peak-to-trough line width close to 19 G and a measured g value of 2.0053. The dark-stable signal found in the P161L mutant (Figure 3d) was more significantly modified compared to the wild type signal II_s spectrum. In the P161L mutant, a 25 G wide and partially resolved multiplet was observed with a zero-crossing at $g = 2.0042$. The sizes (the radicals were quantified in samples (not shown) with constant chlorophyll concentration), on a chlorophyll basis, of the radical signal assigned to Tyr_D^{ox} in all cases were approximately similar (Table 1). In the wild type and two of the mutants, Q164L and P161A, the spin concentration was similar to the PSII concentration as determined by herbicide binding (Table 1). Thus, there was one oxidizable Tyr_D^{ox} per PSII both in the wild type and in the Q164L and P161A mutants. In P161L, the PSII content appeared to be somewhat lower than expected from the size of the radical signal (Table 1). We see two possible reasons for this. Either the rapid photoinactivation and/or the change in the structure of the D2 protein makes some PSII centers unable to bind herbicide or the observed EPR signal is of a composite origin.

Isotopic Labeling and Spectral Simulation. To characterize the modified spectra observed in the mutants (Figure 3), *in vivo* incorporation of specifically deuterated tyrosines were performed in the wild type and in the mutant strains. Figure 4 shows the spectra of the fully protonated form of Tyr_D^{ox} together with the spectra recorded after deuterations in the 3,5-positions or in the β-methylene position from the wild type and two mutants, P161A and Q164L. Due to the smaller gyromagnetic ratio of the deuterium nucleus, exchanging a hydrogen to a deuterium in a free radical will scale the hyperfine splitting from the substituted site by a factor of 1/6.49 (Wertz & Bolton, 1972). Thus, the hyperfine structure observed in a 3,5-deuterated spectrum of a tyrosyl radical is due mainly to interactions between the unpaired spin and the hydrogens at the β-methylene position. On the other hand, upon introducing deuterium at the β-methylene position, the hyperfine couplings to the 3,5-hydrogens will dominate the spectral line shape.

The effects of deuteration on the line shape of the Tyr_D^{ox} spectrum in the wild type and mutants were obvious (Figure 4). Qualitatively, upon deuteration at the β-methylene position the spectra of the wild type and the P161A and Q164L mutants were rather similar, while deuteration at the 3,5-positions of the phenoxy ring emphasized differences between the wild type and mutant spectra. As will be presented in more detail below, this is qualitative evidence that the main reason for the difference between the wild type and P161A/Q164L spectra is related to a modified interaction between the spin at C_1 and the hydrogens associated with the β-methylene carbon. For a more quantitative treatment, the experimental spectra in Figure 4 were analyzed by computer simulation in order to deduce the magnitude of the hyperfine couplings to specific hydrogens of the tyrosine. Using the deuterated spectra we have been able to simulate, with high precision, the spectral line shape of Tyr_D^{ox} from the wild type as well as the altered spectral forms of Tyr_D^{ox} found in the P161A and the Q164L mutants. The simulated spectra are shown below the corresponding experimental spectra in Figure 4. The parameters used to generate the calculated spectra are listed in Table 2. The line shapes in the deuterated spectra were simulated by scaling down the appropriate hyperfine tensors by a factor of 0.154 to account for the gyromagnetic ratio of the deuterium nucleus.

With the hyperfine coupling constants obtained from simulation, the spin density distribution within the tyrosyl radical can be calculated. For hydrogens associated with ring carbons, the isotropic hyperfine coupling constant, A_{iso}, is proportional to the spin density, ρ, at the adjacent carbon (Heller & McConnell, 1960)

$$A_{iso} = Q\rho \qquad (1)$$

where Q is a constant, which for tyrosyl radicals is determined to be –24.9 G (Bender et al., 1989). We initially simulated the spectrum from the wild type which has been experimentally and theoretically studied before (Hoganson & Babcock 1992, 1994). Using isotropic hyperfine coupling values of –6.8 and –6.5 G for the hydrogens bound to the 3,5-positions of the phenoxy ring (Table 2) spin densities at $C_{3,5}$ of 0.26 and 0.27, respectively, were obtained (Table 3). This inequivalence in spin density at symmetrically located carbons in the phenoxy

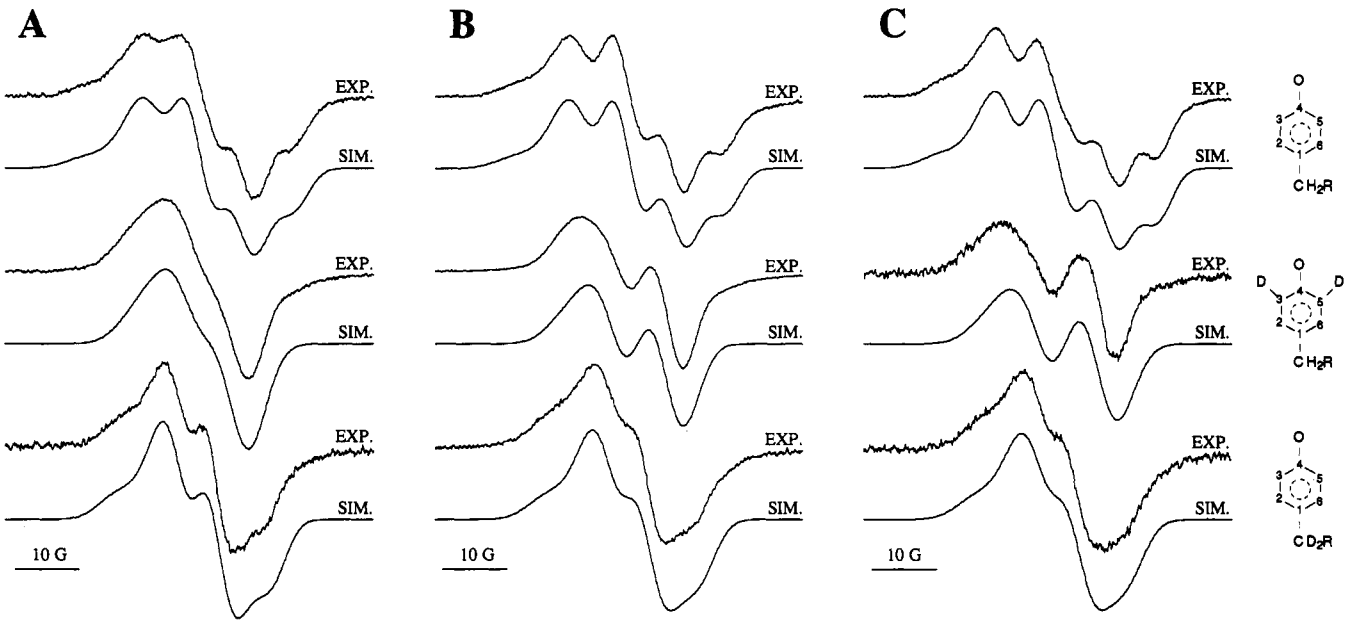

FIGURE 4: EPR spectra from the nondeuterated and specifically deuterated forms of Tyr_D^{ox} in the wild type (A), the P161A mutant (B), and the Q164L mutant (C). Each simulated spectrum is shown immediately below the corresponding experimental spectrum. The parameters used for the simulations are given in Table 2. The upper pairs represent spectra from the nondeuterated form of Tyr_D^{ox}. The middle pairs were obtained after specific deuteration at the 3,5-positions of the phenoxy ring and the bottom pairs after deuteration at the β-methylene position of the tyrosine. All deuterated spectra have been normalized to the same radical concentration as the fully protonated spectrum in the corresponding strain. The numbering of the aromatic moiety of the tyrosine and the isotopically substituted sites are shown to the right. EPR conditions and numbers of scans for each strain were as in Figure 3.

Table 2: Spectroscopic Parameters Used in Simulations of the EPR Spectra of Tyr_D^{ox} in the Wild Type and Site-Directed Mutants of *Synechocystis* 6803

atoms	hyperfine couplings[a]	wild type	P161A	Q164L
C_3–H (C_5–H)	A_x	−10.2	−10.2	−10.1
	A_y	−2.8	−2.8	−2.8
	A_z	−7.3	−7.1	−6.9
	A_{iso}	−6.8	−6.7	−6.6
C_5–H (C_3–H)	A_x	−9.8	−9.7	−9.7
	A_y	−2.8	−2.8	−2.8
	A_z	−6.8	−6.5	−6.5
	A_{iso}	−6.5	−6.3	−6.3
C_1–C_β–H_1	A_x	9.5	10.1	11.5
	A_y	6.5	8.2	9.2
	A_z	6.5	8.2	9.2
	A_{iso}	7.5	8.8	10.0
C_1–C_β–H_2	A_x	3.5	3.4	3.3
	A_y	2.4	1.8	1.5
	A_z	2.4	1.8	1.5
	A_{iso}	2.8	2.3	2.1

[a] The hyperfine couplings are given in gauss. The principal g values used are from Gulin et al. (1992); g_x = 2.00752, g_y = 2.00426, g_z = 2.00212. The hyperfine couplings used to the 2,6-hydrogens are 2.6, 1.6, and 1.6 G. The orientations of the x and y axes of the 3,5- and 2,6-hyperfine tensors relative the corresponding axes of the g tensor are ±23° and ±10°, respectively. The simulations also included a Gaussian line width parameter of 1.8–2.8 G.

ring has recently also been observed using ENDOR spectroscopy of Tyr_D^{ox} from spinach, the green alga *Chlamydomonas reinhardtii*, and the cyanobacterium *Phormidium laminosum* (Table 3; Rigby et al., 1994).

The hyperfine interactions between the unpaired spin and β-methylene hydrogens are, due to the distance, expected to be mainly isotropic and are explained by a hyperconjugation mechanism between the π-electron system on the phenoxy ring and the 1s orbitals of the β-methylene hydrogens (Wertz & Bolton, 1972). Thus, the magnitude of the isotropic coupling depends on both the spin density at C_1 and the dihedral angle between the β-methylene C–H bond and the $2p_z$ orbital at C_1 (see Figure 5, θ_1 and θ_2) according to

$$A_{iso1} \approx \rho_{C1} B \cos^2 \theta_1 \quad (2)$$

$$A_{iso2} \approx \rho_{C1} B \cos^2 \theta_2 \quad (3)$$

$$\theta_2 = \theta_1 + 120° \quad (4)$$

where B is a constant determined to be 58 G (Fassender & Schuler, 1963). Equation 4 is derived assuming an idealized sp^3 hybridization at the β-methylene carbon; thus, the angle (projected on the tyrosine ring plane) between the two C_β–H bonds is 120°.

From the simulations, isotropic couplings of 7.5 and 2.8 G were derived for the two β-methylene hydrogens in the wild type (Table 2). The larger of the β-methylene couplings dominates the 3,5-deuterated spectrum and give rise to the observed doublet (Figure 4A, middle spectrum). Using the two deduced isotropic couplings and the equations above, two possible solutions for the spin density at C_1 and the geometry at the β-methylene position are obtained: ρ_{C1} = 0.34 and θ_1 = 52°, or ρ_{C1} = 0.13 and θ_1 = 173° (see Figure 5, Table 3). These values are in good agreement with those reported in earlier studies of Tyr_D^{ox} in *Synechocystis* sp. (Table 3; Hoganson & Babcock, 1992, 1994).

Solving the electronic structure of Tyr_D^{ox} from the hydrogen hyperfine couplings alone is complicated by the degeneracy in the answer to ρ_{C1}. Two solutions are obtained, ρ_{C1} = 0.34 or 0.13 corresponding to θ_1 = 52° or 173° (Table 3), and it is experimentally difficult to distinguish between these angles. However, in the structural model of PSII the angle corresponding to θ_1 is found to be 40° with a flexibility of approximately ±10° (B. Svensson and S. Styring, unpublished results). Therefore, θ_1 = 52° is a more likely configuration than θ_1 = 173°; thus, the spin density at C_1 most likely is 0.34 and not 0.13. Assuming ρ_{C1} = 0.34 and that the unpaired electron spins add up to unity within the phenoxy ring, we

Table 3: Calculated Spin Density Distribution and Geometry at the β-Methylene Position of the Tyr_D Radical

atoms	*Synechocystis* P161A[a]	*Synechocystis* Q164L[a]	*Synechocystis* wild type[a]	*Synechocystis* wild type[b]	spinach,[c] *C. reinhardtii*,[c] *P. laminosum*[c]
C_1	0.36	0.38	0.34	0.34	0.40
C_3 (C_5)	0.27	0.27	0.27	0.26	0.27
C_5 (C_3)	0.25	0.25	0.26	0.26	0.26
O + C_4[d]	0.28	0.26	0.29	0.30	0.22
θ_1[e,f]	50	48	52	52	48 (spinach) 47 (*C. reinhardtii*) 51 (*P. laminosum*)

[a] This work. [b] From Hoganson and Babcock (1994). [c] From Rigby et al. (1994). [d] The values are calculated assuming spin densities at the $C_{2,6}$ positions of –0.08 and that the spins add up to unity within the phenoxy ring. [e] θ_1 is given in degrees and is defined in Figure 5. [f] A second solution with $\rho_{C_1} = 0.13/\theta_1 = 173°$ for the wild type, $\rho_{C_1} = 0.15/\theta_1 = 179°$ for the P161A mutant, and $\rho_{C_1} = 0.17/\theta_1 = 183°$ for the Q164L mutant is also obtained. However, this solution is disfavored from structural arguments based on the theoretical model (see text; Figure 1).

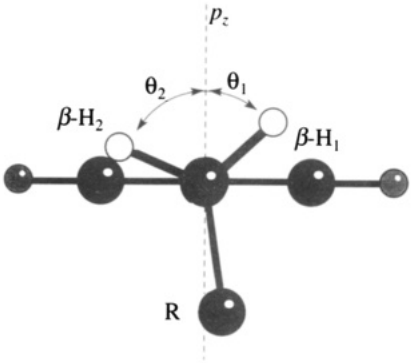

FIGURE 5: Conformation at the β-methylene position of the tyrosine. The plane of the aromatic ring is perpendicular to the plane of the paper; the viewer is looking down the C_β–C_1 bond. The dotted line represents the axis of the $2p_z$ orbital at C_1. θ_1 and θ_2 represent the dihedral angles between the β-methylene C–H_1 and the β-methylene C–H_2 bonds and the $2p_z$ axis at C_1, respectively.

calculate the combined spin density on the oxygen and C_4 to be 0.29 for the wild type. From our data we cannot distinguish how much of the spin that resides at C_4 relative to the amount that resides at the oxygen. However, by a complete analysis of the dipolar tensor of the ring hydrogens of the tyrosyl radical of the *E. coli* ribonucleotide reductase enzyme, Bender et al. (1989) deduced a spin density of –0.03 at the C_4 position. One could expect a similar situation in Tyr_D^{ox}; consequently, the spin at C_4 is expected to be low as compared to the amount residing at the oxygen.

Experimental and simulated EPR spectra of Tyr_D^{ox} obtained on the P161A and Q164L mutants with and without specific deuteration are shown in Figures 4 B,C. The parameters used to obtain the theoretical spectra are listed in Table 2. The resulting spin-density distribution and ring geometry of Tyr_D^{ox} in the two mutants are shown in Table 3. The spectra representing the fully protonated (nondeuterated) Tyr_D^{ox} in the P161A and Q164L mutants were slightly wider and more resolved than the analogous spectrum from wild type (Figures 3 and 4B,C). In fact, the somewhat more resolved spectral line shape representing Tyr_D^{ox} seen in the two mutants are quite similar to the Tyr_D^{ox} spectrum in PSII membranes from spinach (Berthold et al., 1981; Vass & Styring, 1991).

As observed above, upon deuteration at the β-methylene position the spectra of the P161A and Q164L mutants were very similar to the comparable EPR spectrum of wild type thylakoids. This implies that the couplings to the 3,5-hydrogens are altered only slightly by the introduced mutations (Table 2). Indeed, the spin densities at $C_{3,5}$ of 0.25 and 0.27, respectively, in the P161A and Q164L mutants are essentially indistinguishable from the values found for the wild type (Table 3).

Upon introducing deuterium at the 3,5-positions of the phenoxy ring a well-resolved, 16.5 G wide doublet with a 11 G splitting was observed in thylakoids from P161A. The corresponding spectrum from the Q164L mutant was a 18.5 G wide doublet with a splitting of 13 G (Figure 4). The 3,5-deuterated spectra in Figure 4 were dominated by the hyperfine coupling to one of the β-methylene hydrogens (defined as β-H_1 in Figure 5). In the wild type system, the corresponding isotropic value was determined to be 7.5 G (Table 2). In the two mutant strains, our simulations indicate that this interaction is stronger: 8.8 and 10.0 G, for the P161A and Q164L mutants, respectively. These larger couplings result in the wider and more resolved spectra. The weaker coupling to the other β-methylene hydrogen, β-H_2 (Figure 5), was changed only to a minor degree by the mutations (Table 2).

Calculation of the geometry of the phenoxy ring with respect to the β-methylene hydrogens yielded $\theta_1 = 50°$ for P161A and $\theta_1 = 48°$ for Q164L. This is close to the 52° obtained for the wild type system and suggests that a small reorientation of the phenoxy ring has taken place upon mutation of the nearby residues. The spin density at C_1 was increased somewhat for both the P161A and Q164L mutants as compared to wild type (0.36 and 0.38 vs 0.34, respectively). Thus, our results imply that the altered spectral line shapes representing Tyr_D^{ox} in the P161A and Q164L mutants can be explained mainly in terms of increased coupling to β-H_1 by a combination of increased spin density at the C_1 position and a small twist of the phenoxy ring. The changes in the hyperfine coupling to β-H_2 had little effect on the overall spectrum, due to the relative weakness of the coupling.

In Table 3 we have compiled the existing results for the spin density distributions and the geometry at the β-methylene position of Tyr_D^{ox} obtained in eucaryotic systems (spinach and *Chlamydomonas reinhardtii*; Rigby *et al.*, 1994) and in cyanobacteria [*Phormidium laminosum*; Rigby et al. (1994) and *Synechocystis* 6803; this work and Hoganson and Babcock (1994)]. From the accumulated information in these studies it seems clear that alterations in the hyperfine couplings to the β-methylene hydrogens basically determines the spectral line shape of signal II_s. The reported isotropic hyperfine couplings obtained for the 3,5-hydrogens of Tyr_D^{ox} (Table 2; Hoganson & Babcock, 1994; Rigby et al., 1994) are very similar in different species as well as between *Synechocystis* wild type and the two D2 mutants investigated here. Thus, assuming that the value of Q in eq 1 remains constant in the different systems, the spin densities at C_3 and C_5 are similar for Tyr_D^{ox} in the different species studied (Table 3).

Hyperfine interaction between the unpaired spin and a β-H depends on both the magnitude of ρ_{C1} and the degree of hyperconjugation between ρ_{C1} and the β-H as described earlier (eqs 2 and 3). Moreover, due to the geometry dependence

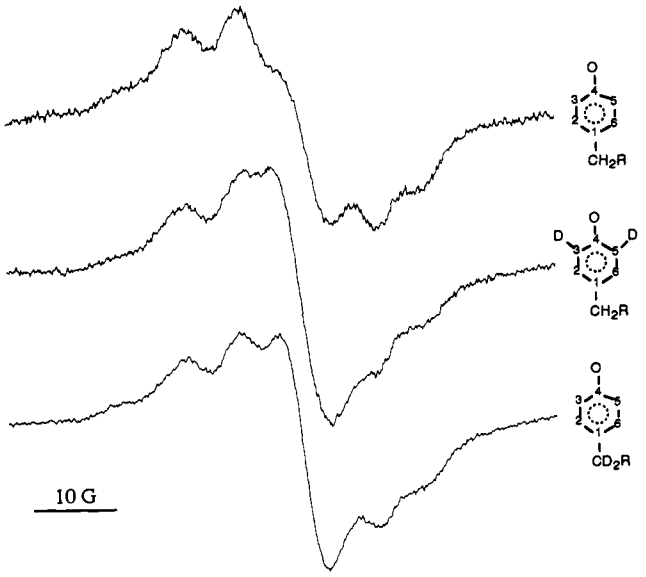

FIGURE 6: EPR spectra of the radical region in the P161L mutant grown on medium with or without the addition of specifically deuterated tyrosine as indicated. EPR conditions: microwave frequency 9.45 GHz; microwave power 63 μW; modulation amplitude 3.3 G; temperature 77 K.

which varies as $\cos^2\theta$, the position of β-H_1 (θ_1, as defined in Figure 5) has a strong influence on the overall line width and hyperfine pattern of signal II_s while β-H_2 has a low impact on the spectrum due to its relative position with respect to the $2p_z$ orbital at C_1 (Figure 5). On the basis of ENDOR studies, Rigby et al. (1994) concluded that the alterations in the β-methylene couplings between different species were only due to slightly different orientations at the β-methylene position and that there were no changes in the spin distribution between different species (Table 3). This is in contrast to the result obtained for the cyanobacterium *Synechocystis* where two independent studies (this work; Hoganson & Babcock, 1994) indicate that the spin distribution actually varies somewhat from that in the other organisms. For wild type *Synechocystis* a value of 0.34 is obtained for ρ_{C1} while Rigby et al. (1994) found a value of 0.40 for ρ_{C1} in all three species investigated (Table 3). Using the spin densities obtained from the hyperfine couplings, a combined value for the spin residing at the oxygen and at C_4 can be calculated if one assumes that the there is, in total, one unpaired electron spin in the ring. For *Synechocystis* the sum of $\rho_O + \rho_{C4}$ is about 0.3 for Tyr_D^{ox} in the wild type and in the mutant strains (Table 3) which is somewhat higher than the value of 0.22 reported by Rigby et al. (1994; also see Table 3).

In the P161L mutant the biochemical situation seemed to be more complex; the mutant was an obligate photoheterotroph; the oxygen evolution was unstable and the PSII content was lowered (Table 1). In addition, the migration pattern of the D2 protein in a denaturing gel system was altered, suggesting a change in the conformation of the protein (Figure 2).

Despite these complications in the P161L mutant, a dark stable radical with spectral properties (high g value, and large line width) similar to those of Tyr_D^{ox}, could be induced (Figure 4). Moreover, the spectrum was sensitive to tyrosine deuteration. Figure 6 shows the dark-stable signal of the P161L mutant grown in normal medium (Figure 6a) and in the presence of specifically deuterated tyrosines (Figure 6b,c). The spectral line shapes obtained after isotopic labeling clearly were altered as compared to the fully protonated spectrum, demonstrating the presence of a tyrosyl radical.

However, while the spectra from Tyr_D^{ox} in the P161A and the Q164L mutants could be simulated well using reasonable assumptions, the situation was not straightforward in the P161L mutant. Although line shape changes were evident upon specific deuteration (Figure 6), the overall line widths of the spectra were essentially insensitive to deuteration. This contrasts with the behavior of Tyr_D^{ox} in wild type and the P161A and Q164L mutants, where deuteration produced spectra with clearly narrowed line widths (see Figure 4). In addition, the multiplet nature of the EPR spectra from the 3,5-deuterated and the β-methylene deuterated samples (Figure 6) are difficult to understand in terms of a tyrosyl radical. Theoretically, the splitting of a spectrum representing a tyrosyl radical could not give rise to the multiplet pattern observed in either of the deuterated samples (Figure 6). The splitting pattern could maximally have a triplet structure in the β-methylene deuterated spectra. In the 3,5-deuterated spectra we could, at most, expect a quartet structure (doublets of a doublet) provided that the β-methylene hydrogens have inequivalent and relatively large couplings. Despite this, the experimentally recorded spectra in both deuterated samples showed multiplet structures more complex than expected (Figure 6b,c) which might indicate that the spectrum observed is not due only to a simple tyrosyl radical.

There are several possible explanations for the behavior described above for the P161L mutant (Figure 6). One is that the deuteration procedure in this mutant resulted in only partial incorporation of the labeled tyrosine. However, the same behavior has been observed in many different preparations of thylakoids from independently grown cultures of P161L including cultures grown to a very low cell density to avoid exhaustion of the added aromatic amino acids. In all other strains, wild type and mutants, our growth protocol resulted in complete incorporation of the labeled tyrosines. However, at present we can not definitively exclude the possibility that metabolic changes in P161L might have altered the incorporation of deuterated tyrosine. Another possibility that we cannot rule out is that the observed signal in the P161L mutant is of a composite origin derived from Tyr_D^{ox} in combination with another species that does not originate from tyrosine since the hyperfine lines are not sensitive to tyrosine deuteration. In this respect it also should be kept in mind that spurious radicals often are observed, especially when the system is somehow perturbed. An third possibility is a structural rearrangement (possibly a covalent crosslinking) of Tyr_D^{ox} that occurs specifically in P161L. This might cause the electron spin to be spread out over a larger number of groups (hence the less-than-expected effects of Tyr deuteration on the EPR spectra in this mutant) and could account for the large proportion of slowly migrating D2 proteins on the gel (Figure 2). Even though at present we are unable to satisfactorily describe all features of the P161L spectrum, our experiments clearly show that, also in this mutant, a tyrosyl radical is present with altered properties as compared to the wild type.

In this paper we have demonstrated how EPR spectroscopy can be employed to determine effects of small changes in the protein environment on the geometry and spin distribution in protein derived tyrosine radicals, here exemplified by Tyr_D^{ox}. The concerted application of various powerful tools, including site-directed mutagenesis, homology-based modeling of the PSII structure and EPR spectroscopy, provides an important avenue to address the question how the protein environment modulates the properties of components involved in photosynthetic electron transfer.

In this respect, the Tyr_D^{ox} radical is particularly suitable because of its easy spectroscopic accessibility and the large variation of Tyr_D^{ox} spectra now available in various site-directed mutants (this paper; Tommos et al., 1993; Tang et al., 1993). Here we have described what structural changes, on the molecular level, might be responsible for the altered spectra. In this respect, it is interesting to note that some mutations induced close to Tyr122 in ribonucleotide reductase (which forms a stable, well understood radical in a protein of which the three-dimensional structure has been determined) also result in modified EPR spectra from the tyrosyl radical (B.-M. Sjöberg, unpublished results). In other mutants, the spectral line shape remains unaltered but the stability and relaxation properties of the radical are altered. Thus, our molecular knowledge of how the protein structure determines the spectral line shape and properties of the tyrosyl radicals increases rapidly, and it will be interesting to compare these relationships between the two systems. It also seems worthwhile to pursue similar studies in other redox enzymes that show radicals derived from amino acid side-chains.

ACKNOWLEDGMENT

Some early work in this project was performed in collaboration with Dr. Bill Rutherford. We acknowledge valuable discussions with Drs. Gerald T. Babcock, Curtis Hoganson, Britt-Marie Sjöberg, and Bengt Svensson. We are grateful to Bengt Svensson for preparation of Figure 1 and to Mr. Torbjörn Astlind for technical assistance. We thank the Department of Biophysics at Stockholm University for the generous access to the EPR spectrometer.

REFERENCES

Andersson, B., & Styring, S. (1991) in *Current Topics in Bioenergetics* (Lee, C. P., Ed.) Vol. 16, pp 1–81, Academic Press, San Diego, CA.

Babcock, G. T. (1987) in *Photosynthesis* (Amesz, J., Ed.), pp 125–158, Elsevier, Amsterdam.

Babcock, G. T., & Sauer, K. (1973) *Biochim. Biophys. Acta 325*, 483–503.

Babcock, G. T., & Sauer, K. (1975) *Biochim. Biophys. Acta 376*, 315–328.

Babcock, G. T., Barry, B. A., Debus, R. J., Hoganson, C. W., Atamian, M., McIntosh, L., & Yocum, C. F. (1989) *Biochemistry 28*, 9557–9565.

Barry, B. A. (1993) *Photochem. Photobiol. 57*, 179–188.

Barry, B. A., & Babcock, G. T. (1987) *Proc. Natl. Acad. Sci. U.S.A. 84*, 7099–7103.

Barry, B. A., El-Deeb, M. K., Sandusky, P. O., & Babcock, G. T. (1990) *J. Biol. Chem. 265*, 20139–20143.

Bender, C. J., Sahlin, M., Babcock, G. T., Barry, B. A., Chandrashekar, T. K., Salowe, S. P., Stubbe, J.-A., Lindström, B., Petersson, L., Ehrenberg, A., & Sjöberg, B.-M. (1989) *J. Am. Chem. Soc. 111*, 8076–8083.

Berthold, D. A., Babcock, G. T., & Yocum, C. F. (1981) *FEBS Lett. 134*, 231–234.

Blankenship, R. E., Babcock, G. T., Warden, J. T., & Sauer, K. (1975) *FEBS Lett. 51*, 287–293.

Boerner, R. J., & Barry B. A. (1993) *J. Biol. Chem. 268*, 17151–17154.

Boussac, A., & Etienne, A.-L. (1984) *Biochim. Biophys. Acta 766*, 576–581.

Brok, M., Babcock, G. T., De Groot, A., & Hoff, A. J. (1986) *J. Magn. Reson. 70*, 368–378.

Debus, R. J., Barry, B. A., Babcock, G. T., & McIntosh, L. (1988a) *Proc. Natl. Acad. Sci. U.S.A. 85*, 427–430.

Debus, R. J., Barry, B. A., Sithole, I., Babcock, G. T., & McIntosh, L. (1988b) *Biochemistry 27*, 9071–9074.

Deisenhofer, J., Epp, O., Miki, K., Huber, R., & Michel, H. (1985) *Nature 318*, 618–624.

Eggers, B., & Vermaas, W. (1993) *Biochemistry 32*, 11419–11427.

Fasanella, E. L., & Gordy, W. (1969) *Proc. Natl. Acad. Sci. U.S.A. 63*, 299–304.

Fassenden, R. W., & Schuler, R. H. (1963) *J. Chem. Phys. 39*, 2147–2195.

Gulin, V. I., Dikanov, S. A., Tsvetkov, Yu. D., Evelo, R. G., & Hoff, A. J. (1992) *Pure Appl. Chem. 64*, 903–906.

Heller, C., & McConnel, H. M. (1960) *J. Chem. Phys. 32*, 1535–1539.

Hoganson, C. W., & Babcock, G. T. (1992) *Biochemistry 31*, 11874–11880.

Hoganson, C. W., & Babcock, G. T. (1994) in *Metal Ions in Biological Systems* (Sigel, H., & Sigel, A., Eds.) Vol. 30, pp 77–100, Marcel Dekker, New York.

Kless, H., Vermaas, W. F. J., & Edelman, M. (1992) *Biochemistry 31*, 11065–11071.

Kraulis, P. J. (1991) *J. Appl. Crystallogr. 24*, 946–950.

MacKinney, G. (1941) *J. Biol. Chem. 140*, 315–322.

Metz, J. G., Nixon, P. J., Rögner, M., Brudvig, G. W., & Diner, B. A. (1989) *Biochemistry 28*, 6960–6969.

Miller, A. F., & Brudvig, G. W. (1991) *Biochim. Biophys. Acta 1056*, 1–18.

Nilsson, F., Gounaris, K., Styring, S., & Andersson, B. (1992) *Biochim. Biophys. Acta 1100*, 251–258.

Rigby, S. E. J., Nugent, J. H. A., & O'Malley, P. J. (1994) *Biochemistry 33*, 1734–1742.

Rippka, R., Deruelles, J., Waterbury, J. B., Herdman, M., & Stanier, R. Y. (1979) *J. Gen. Microbiol. 111*, 1–61.

Ruffle, S. V., Donnelly, D., Blundell, T. L., & Nugent, J. (1992) *Photosynth. Res. 34*, 287–300.

Rutherford, A. W. (1989) *Trends Biochem. Sci. 14*, 227–237.

Sahlin, M., Gräslund, A., Ehrenberg, A., & Sjöberg, B.-M. (1978) *J. Biol. Chem. 257*, 366–369.

Sigel, H., & Sigel, A. (1994) *Metal Ions in Biological Systems*, Vol. 30, Marcel Dekker, New York.

Sjöberg, B.-M., Reichard, P., Gräslund, A., & Ehrenberg, A. (1978) *J. Biol. Chem. 253*, 6863–6865.

Svensson, B., Vass, I., Cedergren, E., & Styring, S. (1990) *EMBO J. 9*, 2051–2059.

Svensson, B., Vass, I., & Styring, S. (1991) *Z. Naturforsch. 46c*, 765–776.

Svensson, B., Etchebest, C., Tuffery, P., Smith, J., & Styring, S. (1992) in *Research in Photosynthesis* (Murata, N., Ed.) Vol II, pp 147–150, Kluwer Academic Publishing, Dordrecht.

Tang, X.-S., Chisholm, D. A., Dismukes, G. C., Brudvig, G. W., & Diner, B. A. (1993) *Biochemistry 32*, 13742–13748.

Tommos, C., Davidsson, L., Svensson, B., Madsen, C., Vermaas, W. F. J., & Styring, S. (1993) *Biochemistry 32*, 5436–5441.

Vass, I., & Styring, S. (1991) *Biochemistry 30*, 830–839.

Vermaas, W. F. J., & Ikeuchi, M. (1991) in *Cell Culture and Somatic Genetics of Plants* (Bogorad, L., & Vasil, I. K., Eds.) Vol. 7B, pp 25–111, Academic Press, San Diego.

Vermaas, W. F. J., Rutherford, A. W., & Hansson, Ö. (1988a) *Proc. Natl. Acad. Sci. U.S.A. 85*, 8477–8481.

Vermaas W. F. J., Ikeuchi, M., & Inoue, Y. (1988b) *Photosynth. Res. 17*, 97–113.

Vermaas, W. F. J., Charité, J., & Eggers, B. (1990a) in *Current Research in Photosynthesis* (Baltscheffsky, M., Ed.) Vol. I, pp 231–238, Kluwer, Dordrecht, The Netherlands.

Vermaas, W. F. J., Charité, J., & Shen, G. (1990b) *Z. Naturforsch. 45c*, 359–365.

Vermaas, W. F. J., Charité, J., & Shen, G. (1990c) *Biochemistry 29*, 5325–5332.

Vermaas, W. F. J., Styring, S., Schröder, W., & Andersson B. (1993) *Photosynth. Res. 38*, 249–263.

Wertz, J. E., & Bolton, J. R. (1972) *Electron Spin Resonance, Elementary Theory and Practical Applications*, Chapman and Hall, New York.

Yu, J., & Vermaas, W. F. J. (1993) *J. Biol. Chem. 268*, 7407–7413.